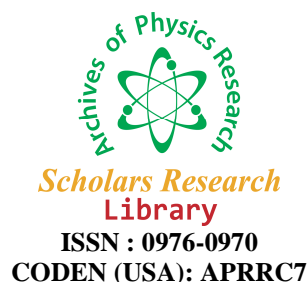




## Scholars Research Library

Archives of Physics Research, 2012, 3 (2):156-164  
(<http://scholarsresearchlibrary.com/archive.html>)



### Shapes of Multiple-Beam Fizeau Fringes Crossing D-shaped and Quasi-D-shaped Optical Fibers

M. M. El-Nicklawy<sup>1</sup>, R. M. El-Agmy\*<sup>1,2</sup>

<sup>1</sup>Helwan University, Faculty of Science (Physics)11792-Helwan-Egypt  
<sup>2</sup>Department of Physics, Taif University, PO Box 888, Taif, Saudi Arabia

#### ABSTRACT

Mathematical expressions for multiple-beam Fizeau fringes crossing D-shaped and quasi-D-shaped optical fiber are derived. The numerical simulations for the derived equations at different optical fiber rotations angles are presented. The numerical simulations of the derived equations of quasi-D-shaped optical fibers are verified experimentally.

#### INTRODUCTION

Rare-earth ions doped fiber lasers have attracted much attention due to absence of thermal problems, high power, single mode emission and high conversion efficiency. Because of that rare-earth-doped fiber lasers are one of the most attractive laser devices for applications in sensors, biochemical sensing [1], optical communications, and industrial applications. High conversion efficiency is reached by increasing the absorption of pump light into fiber core. More precisely, the absorption depends on the transversal mode structure in the inner cladding and the fiber geometry [2, 3]. In order to increase the absorption of the pump light, it is desirable to have an eccentric core in a noncircular cladding to absorb higher order modes [4].

To date, there are a variety of cladding geometries to improve pump absorption, e.g., circular offset, rectangular, flower, and a circular cladding with an inner D-shaped [5-10]. D-shaped fiber lasers has been widely used in high-power double-clad fiber lasers because of its high pump absorption efficiency and low production cost as compared with rectangular and circular offset core cross-sectional fibers [11], even when using a multimode pump source [12-13]. Refractive indices of the fiber core-cladding and core diameter are the basic transmission parameter. Adjustment of these parameters is major of interest during and after manufacturing process. Different techniques have been used to determine refractive indices and core-cladding dimensions [14-18]. Two beam and multiple beam interference methods applied to fibrous material has been discussed extensively [19-22]. In this work mathematical expressions for multiple-beam Fizeau fringes crossing D-shaped and quasi-D-shaped optical fiber are derived. The numerical simulations for the derived equations at different optical fiber rotations angles are presented. The numerical simulations of the derived equations of quasi-D-shaped optical fibers are verified experimentally.

#### 2. Theoretical Considerations

##### 2.1. Quasi-D-Shaped optical fiber

The theoretical model is driven based on an electron micrograph of the fiber as shown in Fig. 1 [4]. Consider a fiber of elliptical core of radii  $a$  and  $b$ , two crossed circles of radii  $R_1$  and  $R_1$  to form quasi-D-Shaped cladding as shown in Fig. 2. Let the fiber core of refractive index  $n_c$  and its cladding of refractive index  $n_s$  be introduced in a silvered liquid wedge of refractive index  $n_L$  with wedge angle  $\epsilon$ .

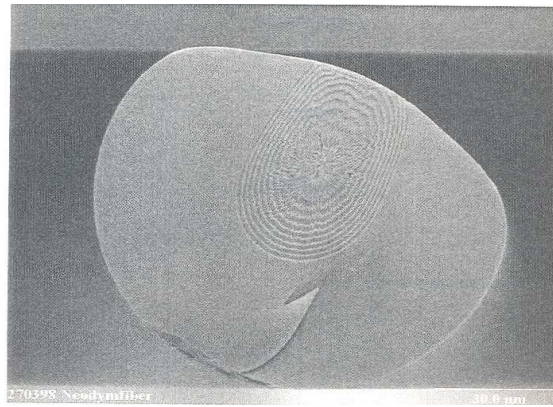


**Fig.1.** Scanning electron microscope picture of the fiber [4].

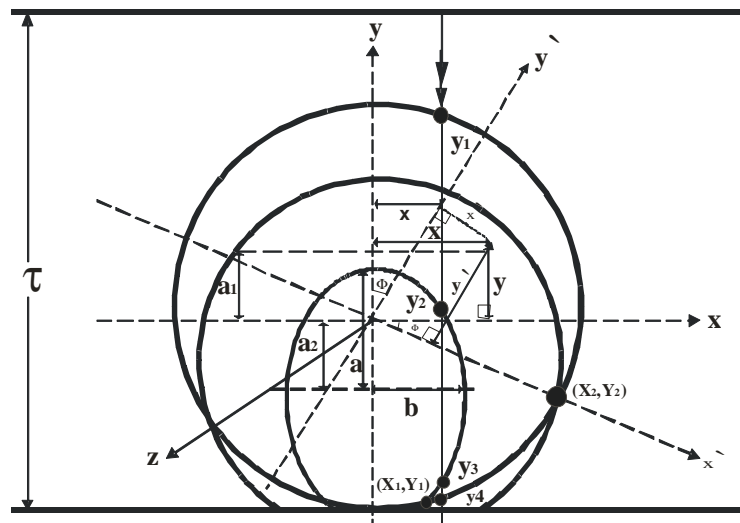


**Fig. 2.** Cross-section of a fiber having an elliptical core, with a refractive index  $n_c$ , shifted away from the centre of a skin of quasi-D-shaped of radii  $R_1$  and  $R_2$ , of refractive index  $n_s$ , immersed in a silvered liquid wedge of refractive index  $n_L$  [5].

Let the setting of the fiber be such that its axis (the z-axis) is perpendicular to the edge of the wedge (the x-axis). A monochromatic light beam of wavelength  $\lambda$  traverses the fiber parallel to the major radius of its core. The optical path length, OPL, through the x-y plane, (Fig. 2) will be given by [5]:

$$OPL = n_L t + (y_1 - y_2)(n_s - n_L) + (y_2 - y_3)(n_c - n_L) + (y_3 - y_4)(n_s - n_L) \tag{1}$$

Where  $t = z \tan \epsilon$ .

$$y_1 = (R_1^2 - x^2)^{1/2} \tag{2}$$

$$y_2 = a \sqrt{1 - \frac{x^2}{b^2}} - a_2 \tag{3}$$

$$y_3 = -a \sqrt{1 - \frac{x^2}{b^2}} - a_2 \tag{4}$$

$$y_4 = -\sqrt{R_2^2 - x^2} + a_1 \tag{5}$$

where  $R_1$  and  $R_2$  are the radii of the fiber and  $a$  and  $b$  are the major and minor radii of the elliptical core, respectively.

For a fringe of interference of order  $N$  we get:

$$N\lambda = 2[n_L t_N + (y_1 - y_2)(n_s - n_L) + (y_2 - y_3)(n_c - n_L) + (y_3 - y_4)(n_s - n_L)] \quad (6)$$

Transforming the origin to  $\left(0, \frac{N\lambda}{2n_L \tan \varepsilon}\right)$  on the  $x - z$  plane gives:

$$n_L z \tan \varepsilon = (y_1 - y_2)(n_s - n_L) + (y_2 - y_3)(n_c - n_L) + (y_3 - y_4)(n_s - n_L) \quad (7)$$

The ratio between the fringe shift  $dz$ , and the fringe spacing  $\Delta z$  expressed by:

$$\Delta z = \frac{\lambda}{2n_L \tan \phi} \quad (8)$$

is given by:

$$\frac{dz}{\Delta z} = \frac{2}{\lambda} [(y_1 - y_2)(n_s - n_L) + (y_2 - y_3)(n_c - n_L) + (y_3 - y_4)(n_s - n_L)] \quad (9)$$

Equation (9) is applicable only for the following conditions, where:

$$y_1 \xrightarrow{\text{in-the-range}} -R_1 \leq x \leq R_1;$$

$$y_2 \xrightarrow{\text{in-the-range}} -b \leq x \leq b;$$

$$y_3 \xrightarrow{\text{in-the-range}} -\sqrt{R_2^2 - (Y_1 - a_1)^2} \geq x \geq \sqrt{R_2^2 - (Y_1 - a_1)^2} \text{ and}$$

$$y_4 \xrightarrow{\text{in-the-range}} -X_2 \leq x \leq X_2$$

$X_2$  and  $Y_1$  are given by:

$$Y_1 = \frac{-B \pm \sqrt{B^2 - 4AC}}{2A} \quad (10)$$

$$\text{where, } A = \frac{1}{a^2} + \frac{1}{b^2}, B = 2\left(\frac{a_1}{b^2} + \frac{a_2}{a^2}\right) \text{ and } C = \frac{R_2^2}{b^2} - \frac{a_1^2}{b^2} + \frac{a_2^2}{a^2} - 1$$

$$X_2 = \pm \sqrt{R_1^2 - \left\{ \frac{a_1^2 (R_2^2 - R_1^2)}{2a_1} \right\}^2} \quad (11)$$

By rotating the fiber by an angle  $\Phi$  the new coordinates are given by:

$$\begin{cases} x = y' \sin \phi + x' \cos \phi \\ y = y' \cos \phi - x' \sin \phi \end{cases} \text{ or } \begin{cases} x' = x \cos \phi - y \sin \phi \\ y' = x \sin \phi + y \cos \phi \end{cases} \quad (12)$$

### 2.1. D-Shaped optical fiber

Consider a fiber of circular core of radius  $r_c$  and skin of radius  $r_s$ , the skin has D-Shaped as shown in Fig. 3. Let the fiber core of refractive index  $n_c$  and its cladding of refractive index  $n_s$  be introduced in a silvered liquid wedge of refractive index  $n_L$  with wedge angle  $\varepsilon$ .

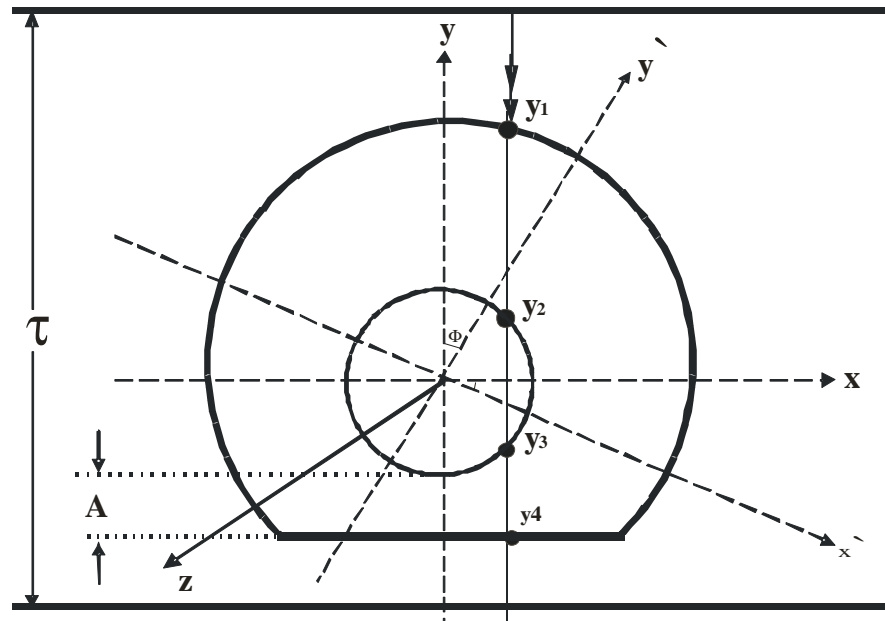


**Fig. 3.** Cross-section of a D-shaped fiber immersed in a silvered liquid wedge of refractive index  $n_L$ .

Let the setting of the fiber be such that its axis (the z-axis) is perpendicular to the edge of the wedge (the x-axis). A monochromatic light beam of wavelength  $\lambda$  traverses the fiber parallel to the major radius of its core. The optical path length, OPL, through the x-y plane, (Fig. 3) will be given by:

$$OPL = n_L t + (y_1 - y_2)(n_s - n_L) + (y_2 - y_3)(n_c - n_L) + (y_3 - y_4)(n_s - n_L) \tag{13}$$

Where  $t = z \tan \epsilon$ .

$$y_1 = (r_s^2 - x^2)^{1/2} \tag{14}$$

$$y_2 = (r_c^2 - x^2)^{1/2} \tag{15}$$

$$y_3 = -(r_c^2 - x^2)^{1/2} \tag{16}$$

$$y_4 = A \tag{17}$$

For a fringe of interference of order  $N$  we get:

$$N\lambda = 2[n_L t_N + (y_1 - y_2)(n_s - n_L) + (y_2 - y_3)(n_c - n_L) + (y_3 - y_4)(n_s - n_L)] \tag{18}$$

Transforming the origin to  $\left(0, \frac{N\lambda}{2n_L \tan \epsilon}\right)$  on the  $x - z$  plane gives:

$$n_L z \tan \epsilon = (y_1 - y_2)(n_s - n_L) + (y_2 - y_3)(n_c - n_L) + (y_3 - y_4)(n_s - n_L) \tag{19}$$

The ratio between the fringe shift  $dz$ , and the fringe spacing  $\Delta z$  expressed by:

$$\Delta z = \frac{\lambda}{2n_L \tan \phi} \tag{20}$$

is given by:

$$\frac{dz}{\Delta z} = \frac{2}{\lambda} [(y_1 - y_2)(n_s - n_L) + 2 \cdot (y_2 - y_3)(n_c - n_L) - y_3 \cdot (n_s - n_L)] \tag{21}$$

Equation (21) is applicable only for the following conditions, where:

$$\begin{aligned}
 y_1 &\xrightarrow{\text{in-the-range}} -r_c < x < r_s; \\
 y_2 &\xrightarrow{\text{in-the-range}} r_c < x < r_c; \\
 y_3 &\xrightarrow{\text{in-the-range}} -r_c < x < r_c \text{ and} \\
 y_4 &\xrightarrow{\text{in-the-range}} -r_c < x < r_c
 \end{aligned}$$

By rotating the fiber by an angle  $\Phi$  the new coordinates are given by:

$$\left\{ \begin{aligned} x &= y' \sin \phi + x' \cos \phi \\ y &= y' \cos \phi - x' \sin \phi \end{aligned} \right\} \text{ or } \left\{ \begin{aligned} x' &= x \cos \phi - y \sin \phi \\ y' &= x \sin \phi + y \cos \phi \end{aligned} \right\} \tag{22}$$

**MATERIALS AND METHODS**

**3. Experimental setup:**

The optical set up for producing multiple-beam Fizeau fringes in transmission is shown in figure 4. A parallel beam of monochromatic light is incident normally on the wedge interferometer placed on a microscope stage. The wedge interferometer consists of two circular partially reflecting optical plates having diameter of 4.5 cm, 19 mm thickness and flat to  $\pm 0.01$  micron, the reflection coefficient of the upper mirror and lower mirror are about 80% and 75%, respectively. The coating was prepared by thermal evaporation of spec-pure silver in a vacuum better than  $10^{-4}$  torr, to produce multiple-beam Fizeau fringes in transmission, the wedge is illuminated as seen from figure 1, from the lower side i.e. the side of the horizontal mirror.

A drop of liquid with a refractive index ( $n_l$ ) close to that of the most outer fiber’s skin was put on the silvered face of the lower optical flat as immersion liquid (mixture of  $\alpha$  – promonaphthalene and paraffin oil). The fiber was immersed in the liquid and the upper optical flat was then introduced to form the wedge interferometer. Both the gap thickness and the wedge angle can be adjusted to form the sharpest fringes normal to the fiber. A polarizer was inserted in the path of monochromatic beam to allow the incident beam of light to vibrate either parallel or perpendicular to the fiber axis.

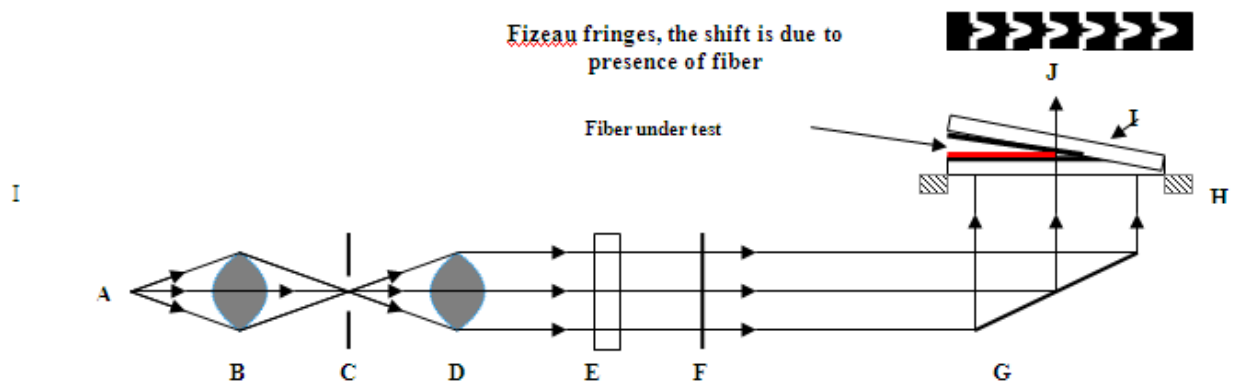


**Fig. 4. Optical arrangements for producing multiple-beam Fizeau fringes, in transmission where, A-Mercury lamp, B- Condenser lens, C- Iris diaphragm, D- Collimating lens, E- Polarizer F- Monochromatic filter, G- Reflecting mirror, H- Microscope stage, I- Silvered liquid wedge interferometer, J- To the Microscope.**

**4. Modeling and experimental results**

**4.1 Quasi-D-Shaped fiber**

Shapes of Multiple-beam Fizeau fringes crossing quasi-D-shaped fibers are obtained by solving equation (9). The parameters that used in solution are given in table I.

**Table I** constant that used for quasi-D-shaped fiber modeling [5]

$n_L$	$n_s$	$n_c$	$R_1$	$R_2$	a	b	$a_1, a_2$	$\lambda$
1.4607	1.4604	1.4609	$1.1 \cdot R_2$	48.19 $\mu\text{m}$	20.9 $\mu\text{m}$	7.708 $\mu\text{m}$	12.85 $\mu\text{m}$	546.1 nm

Fig. 5 shows numerical modeling simulation results of different shaped of multiple-beam fizeau fringes crossing quasi-D-shaped fiber at different rotations angles (a) 0°, (b) 30°, (c) 60° and (d) 90°.

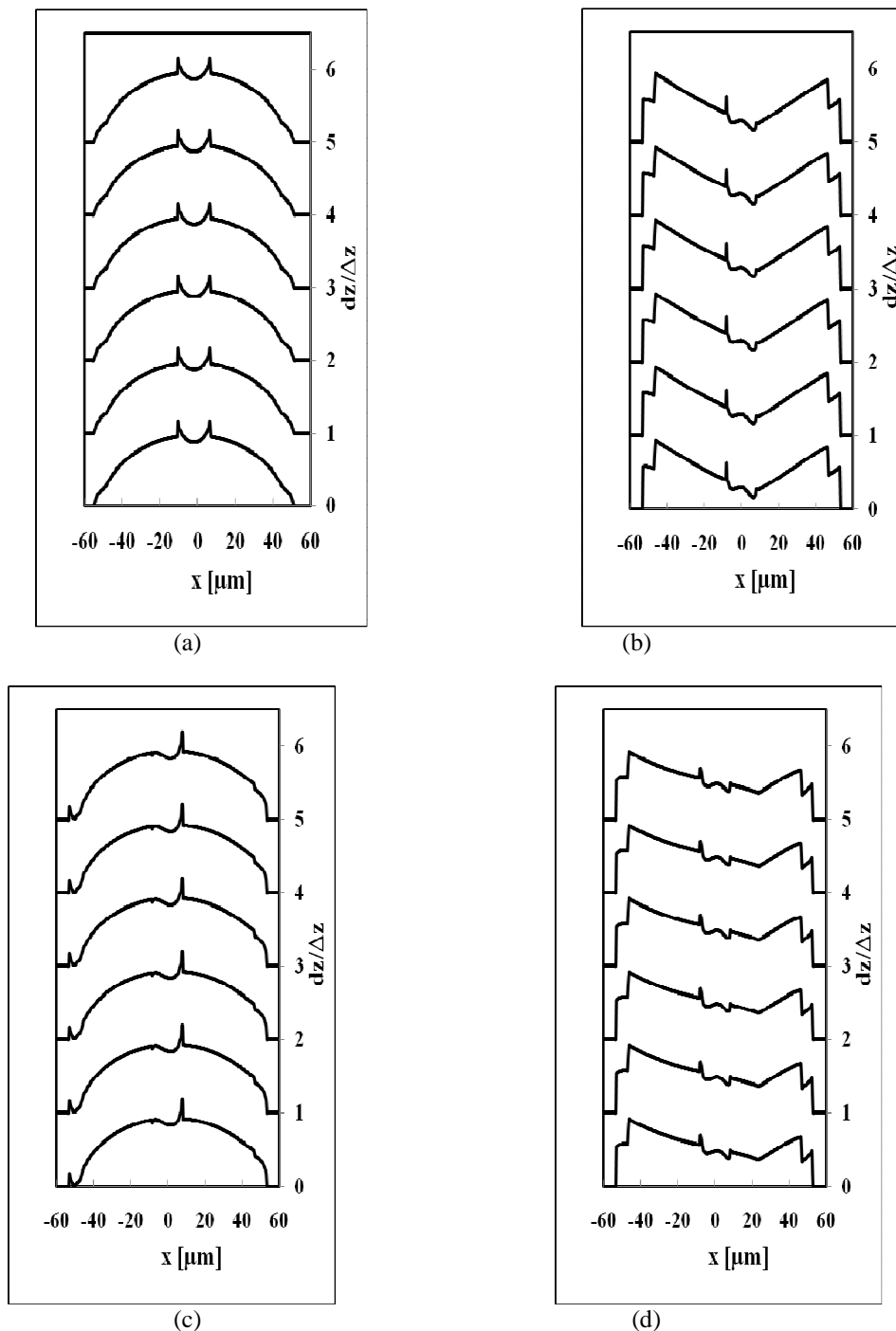
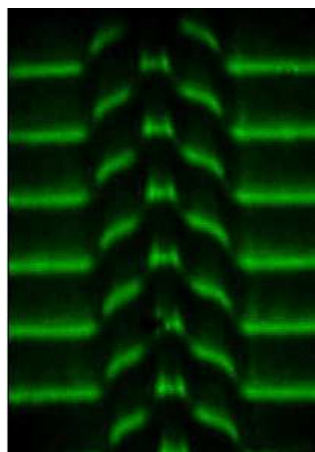


Fig.5 Shows calculated  $\left[ \frac{dz}{\Delta z} \right]$  shapes of multiple-beam Fizeau fringes crossing quasi-D-shaped fibers with different rotation angles (a) (a) 0°, (b) 30°, (c) 60° and (d) 90°.

Fig. 6 shows the microinterferogram (experimental) of multiple-beam Fizeau fringes crossing the quasi-d-shaped fiber. Table II gives the experimental values of the refractive indices of the cladding and core.



**Fig. 6 Microinterferograms of multiple-beam Fizeau crossing quasi-D-shaped fiber.**

The measured microinterferograms is in a good agreement with the calculated results shown with rotation angle of  $0^\circ$  as shown in fig. (5a) [5].

**Table II Values of refractive indices of the quasi-D-shaped fiber**

Temperature $^\circ\text{C}$	Wavelength nm	$n_L$	$n_s$	$n_c$
25	456.1	1.4605	1.4602	1.612

#### 4.2 D-Shaped fiber

Shapes of Multiple-beam Fizeau fringes crossing D-shaped fibers are obtained by solving equation (21). The D-shaped fiber geometry was taken from fig. 7. [2004]. The parameters that used in solution are given in table III.

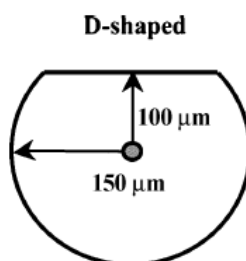


**Fig. 7 shows draw of d-shaped optical fiber [11]**

**Table III constant that used for quasi-D-shaped fiber modeling**

$n_L$	$n_s$	$n_c$	$r_s$	$r_c$	a	$\lambda$
1.4603	1.4604	1.4607	75 $\mu\text{m}$	2.5 $\mu\text{m}$	100 $\mu\text{m}$	546.1 nm

Fig. 8 shows numerical modeling simulation results according to equation (21), of different shaped of multiple-beam fizeau fringes crossing D-shaped fiber at different rotations angles (a)  $0^\circ$ , (b)  $30^\circ$ , (c)  $60^\circ$  and (d)  $90^\circ$ .

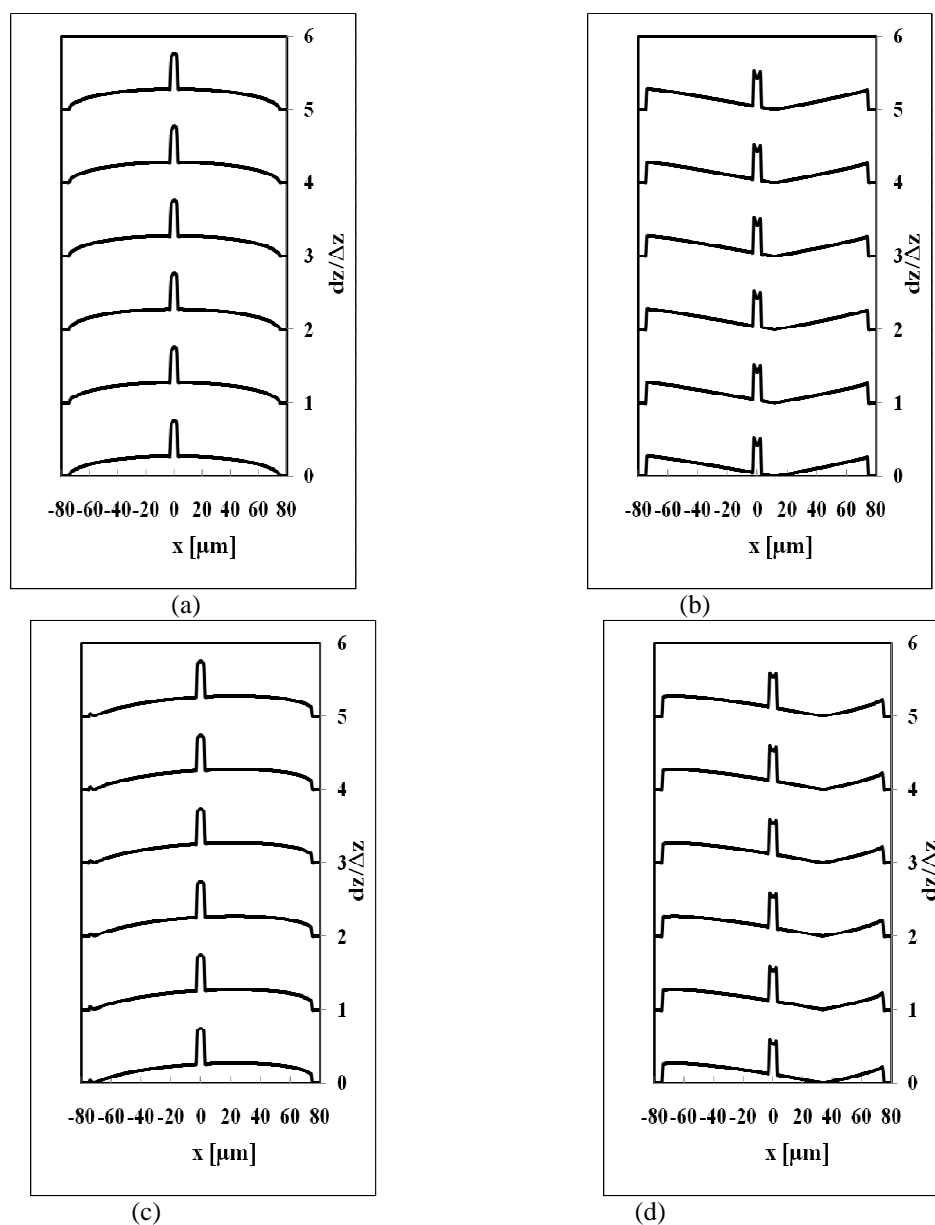


Fig.8 Shows calculated  $\left[ \frac{dz}{\Delta z} \right]$  shapes of multiple-beam Fizeau fringes crossing quasi-D-shaped fibers with different rotation angles (a) (a)  $0^\circ$ , (b)  $30^\circ$ , (c)  $60^\circ$  and (d)  $90^\circ$ .

### CONCLUSION

In conclusion we have derived a new mathematical formula for multiple-beam Fizeau fringes crossing D-shaped fiber. Numerical calculations for quasi-D-shaped and D-shaped optical fibers at different rotation angles inside the interferometer are presented. Good agreement between the theoretical and experimental results for quasi-D-shaped fiber is given. This work is very useful for quality control for producing such fibers. The adjustment of the three basic transmission parameters refractive indices of core and cladding and core diameter are major of importance.

### REFERENCES

- [1] Ch. Chen, et.al., *J. of laser micro/noneng.*, 6 (1), 81 (2001).
- [2] S. Bedo, W. Luthy, H. P. Weber, *Opt. Comm.*, 99, 331 (1999).
- [3] S. D. Jackson, M. Ahmed, T. A. King, Abstract Book, Proc. SPIE, 2629, 169 (1996).
- [4] R. Renner, M. Kehrl, W. Lüthy, and H. P. Weber, *Laser Physics*, 13 (2), 233 (2003).



- [5] M. M. El-Nicklawy, R. M. El-Agmy, A. F. Hassan, M. El-Hagary, A. Adel, *Egyptian J. of Solids*, 32 (1), 45 (2009).
- [6] P. Leproux, S. Fevrier, V. Doya, P. Roy, and D. Pagnoux, *Opt. Fiber Technol.*, 6, 329 (2001).
- [7] Martinez-Rios, A. N. Starodumov, H. Po, Y. Wang, A. A. Demidov, and X. Li, *Opt. Lett.*, 28 (18), 1642 (2003).
- [8] H. Zellmer, A. Tünnermann, H. Welling, and V. Reichel, in *Optical Amplifiers and Their Applications*, Optical Society America, Trends Optics and Photonics (OSATOPs), 16, 137 (1997).
- [9] J. Nilsson, S. Alam, J. A. Alvarez-Chavez, P.W. Turner, W. A. Clarkson, and A. B. Grudinin, *IEEE J. Quantum Electron.*, vol. 39, 987 (2003).
- [10] E. M. O'Brien and C. D. Hussey, *Electron. Lett.*, 35 (2), 168 (1999).
- [11] Li. Yahua, S. D. Jackson, S. Fleming, *IEEE Photonics Technology Letters*, 16 (11), 2502 (2004).
- [12] R. EL-Agmy, W. Luethy, Th. Graf, H. P. Weber, *Appl. Phys. B*, 67, 23 (2003).
- [13] R. EL-Agmy, W. Luethy, Th. Graf, H. P. Weber, *Electronics letters* 39 (6), 507 (2003).
- [14] R. C. Faust, *Proc. Phys. Soc.*, 67, 138 (2008).
- [15] S. M. Betrabet, K. P. R. Pillay and R. L. N. Lyendar, *Text. Res. J.* 33, 720 (1963).
- [16] A.A. Hamza, A.E. Belal, T.Z.N. Sokkar, H.M. EL-Dessouky, M.A. Agour, *Optics and Lasers in engineering*, 45 (1), 145 (2007).
- [17] E.A. Galperin, *Computers & Mathematics with Applications*, 56 (5), 1271 (2008).
- [18] M. J. Pluta, *Microsc.* 96, 309 (1971).
- [19] N. Barakat, A. A. Hamza, „*intrferometry of fibrous materials*“, Adam Higler, Brisol, 1990.
- [20] Xiaojun Cao, Jianqiang Zhu, Yanhong Li, Qiang Lin, *Optik - International Journal for Light and Electron Optics*, 118 (10), 495 (2007).
- [21] M. M. El-Nicklawy, I. M. Fouda, *J. Text. Inst.* 71, 252 (1980).
- [22] Sanjib Chatterjee, Y. Pawan Kumar, *Optics & Laser Technology*, 39 (3), 662 (2007).
- M. M. El-Nicklawy, I. M. Fouda, *J. Text. Inst.* 71, 257 (1980).